Residual Stress Enhancement of X-2M Foreign Object Damage Tolerance

John E. VanDalen, Marc E. Hopkins, Michael R. Hill

Mechanical and Aerospace Engineering, University of California, Davis, CA 95616 USA

Abstract
The objective of this paper is to quantify the effects of residual stresses imparted by laser shock peening on the foreign object damage (FOD) tolerance of X-2M, a high-strength, carburized steel used for gears. Tests were performed on simple blocks of material to characterize residual stresses from carburization and from laser shock peening. Fatigue tests were performed in bending on bars of material containing a notch representative of observed FOD. The fatigue test results show that laser shock peened coupons have significantly improved performance, with peened coupons having about twice the fatigue strength of as-carburized coupons.

Keywords Carburized steel, residual stress, foreign object damage, fatigue

Introduction

Foreign object damage (FOD) occurs when a hard piece of debris (rock, sand, shrapnel, etc.) traveling at a high velocity strikes the surface of a component resulting in damage to the surface in the form of a notch. This damage acts as a stress concentration and can lead to early fatigue crack initiation and potentially premature failure of the component [1, 2, 3]. A great deal of research has been conducted to investigate FOD effects on aircraft turbine engines and turbo machinery, in which the compressor blades are particularly susceptible to FOD due to ingestion of debris. Fatigue failure initiated by FOD can occur in other systems as well, like rotorcraft transmissions, and this study will investigate such a case. Current literature indicates that a deep surface layer of compressive residual stress imparted by methods such as low plasticity burnishing and laser shock peening (LSP) can significantly improve the fatigue performance of a component subjected to FOD post-treatment [4, 5, 6, 7].

Laser shock peening was chosen for investigation in this study because it is an emerging surface treatment that is used to improve material performance [4,8]. Like other similar surface treatments, laser shock peening produces a layer of compressive residual stress near the surface of a part. Since applied stresses are superimposed with residual stress produced by laser shock peening, and since fatigue damage is related to the mean value of the cyclic stress history, the compressive residual stress from laser shock peening can improve fatigue performance by prolonging time to crack initiation and slowing crack growth. Since compensating tensile residual stresses will develop as a result of the residual stress treatment (to satisfy equilibrium within the body), care must be taken to ensure that these tensile stresses develop in non-critical locations and do not adversely affect performance.

The primary objective of this paper is to illustrate the effects of residual stresses imparted by laser shock peening on the FOD tolerance of X-2M, a high-strength, carburized steel used for gears.

Methods

The objective of this study was accomplished by comparing coupons in two conditions: as-carburized (AC) and laser shock peened (LP), both of which contained simulated FOD. Residual stresses existing in the material due to carburization and laser shock peening were measured via the slitting method. Coupons were then exposed to three-point bend fatigue loading to evaluate their performance.

X-2M is a carburized gear steel that has greater scuffing (scoring) resistance and greater pitting (surface fatigue) resistance than carburized 9310 steel. X-2M is used in military rotorcraft transmission gears and was therefore selected as the material of interest for this study. The chemical composition of X-2M is shown in Table 1 and mechanical properties of the core material are listed in Table 2 [9]. The material was received as 133.4 mm diameter, 9.5 mm thick discs removed from 133.4 mm diameter round bar stock. The top and bottom faces, normal to the long direction of the bar stock, were carburized by the supplier [9]. Grain size varied radially out from the center of the discs. The potential effects of this were accounted for by tracking coupon location and creating two identical sets of coupons, based on location (Figure 1, Table 3).

Two types of coupons were utilized in this study; residual stress and fatigue. All of the coupons were cut from the parent material using wire electric discharge machine (EDM), and fatigue coupons were lightly ground on the EDM cut sides to remove the recast layer. Residual stress coupons were blocks, 25.4 mm by 19.1 mm in the plane of the disc and 9.5 mm thick (Figure 2). Two RS coupons were used, one AC and one LP, to determine residual stress in each condition. Fatigue coupons were bars, 76.2 mm long with rectangular cross section 9.5 mm wide and 6.35 mm thick (Figure 3). Ten fatigue coupons were utilized, five in each condition, AC or LP.

FOD was simulated with a small triangular notch machined into each coupon using a plunge EDM. The location and dimensions of the simulated FOD are illustrated in Figure 3. Dimensions for the simulated FOD were chosen to be representative of potential in-service surface damage. Notches were machined into LP coupons after peening to simulate in-service, post-peening, damage.

A blank of material for LP coupons was removed from the parent material, laser shock peened, and then sectioned into individual coupons. Laser shock peening was applied using a flash lamp pumped Nd:glass slab laser system capable of 1 to 30 ns pulse durations at irradiances of 1 GW/cm^2 to 12 GW/cm^2. The footprint of the laser spot is rectangular, allowing for uniform coverage of the desired treatment area. Prior to laser shock peening, a sacrificial ablative layer is applied to the surfaces of the part to be treated. The pressure resulting from the ablation of this layer is confined to the surface of the part by a thin film of water (inertial tamping layer). For this study, an aluminum adhesive tape was used as the ablative layer. This tape is removed and replaced between peening layers, because it is consumed during the peening process. Laser shock peening was applied spot by spot, line by line, over the entire top surface of the material to be used for the LP coupons. Based on previous work in 300M [10], a through hardened high-strength steel, the laser shock peening treatment parameters selected for this study were 10 GW/cm^2 irradiance, 18ns pulse duration and 3 layers (300% coverage).

The slitting method (also know as the crack compliance method) was employed to measure the residual stress distribution as a function of depth from the treated surface. This method was introduced by Vaidyanathan and Finnie and was recently reviewed by Prime [11, 12]. In this method, a slit is incrementally extended into a body containing residual stress using a precise and gentle machining process, most often wire EDM. As residual stresses are released on the traction free surfaces of the slit, the body deforms. This deformation is measured with a strain gage placed on the surface opposite the one of interest, directly in-line with the slit. The released strain is input into an inverse elastic analysis based on a compliance matrix derived from finite element analysis of the coupon. The inverse elastic analysis determines a profile of residual stress as a function of depth from the surface that corresponds to the measured strain. Further details on this method have been omitted for brevity but can be found in Lee and Hill [13]. Residual stress profiles were measured for both the AC and LP conditions because significant residual stress is expected in both condtions.

Fatigue testing was conducted on a computer controlled servo hydraulic load frame. Coupons were loaded in three-point bending, as shown in Figure 4, and subjected to constant amplitude fatigue loading with an applied stress ratio of 0.1 and a test frequency of 12 Hz. Initial stress levels were selected in order to obtain failure in the 750,000 to 1,000,000 cycle range, and then adjusted based on initial results. Each stress level was dynamically calibrated using a strain gaged AC coupon with no notch. Failure was defined as a 200% change in the compliance of the coupon. Runout was defined when a coupon reached 1,000,000 cycles without failure.

Results

The results from residual stress measurements are shown in Figure 5. As expected, significant levels of compressive residual stress are present within the carburized layer of the AC X-2M. LP was able to induce an additional 700 MPa of compressive residual stress near the surface and increased the depth of the compressive zone from 1.8 mm to 2.0 mm.

The fatigue test results, Figure 6, demonstrate that LP significantly improved the damage tolerance of X-2M material. For the size of simulated FOD defect tested here, the LP coupons failed at about twice the level of applied stress as the AC coupons, for the same life. One of the LP coupons failed away from the FOD notch and is not included in the reported data.

No correlation between coupon location in the parent material and fatigue lifetime was observed.

Discussion

Residual stress treatment of this material provided significant improvement in fatigue performance. In order to better understand the role of residual stress in these tests, LEFM was used to predict fatigue crack growth behavior in the coupons. The analysis used the publicly available software program AFGROW. FOD was modeled as a semi-elliptic surface crack having initial depth and width corresponding to the dimensions of the machined notch. A weight function solution was employed in order to include the measured RS profiles, which were assumed to vary only with depth from the surface. Baseline fatigue crack growth (FCG) data was not available for X-2M, and so a Walker Equation correlation for 300M was used in the predictions (Eqn 1-4), where coefficients were developed from data in Mil Handbook 5G by Pistochini [10], and are $C = 9.63\times10^{9}$ (mm/cycle)/(MPa$\sqrt{m}$)^n, n = 2.99, and m = 0.68.

$$da/dN = C(\Delta K_w)^n \quad (1)$$

$$R = (K_{app,min} + K_{RS})/(K_{app,max} + K_{RS}) \quad (2)$$

$$\Delta K_w = (K_{app,max} - K_{app,min})(1 - R)^{(m-1)} \quad \text{for } R \geq 0 \quad (3)$$

$$\Delta K_w = K_{app,max} + K_{RS} \quad \text{for } R < 0 \quad (4)$$

Sample fracture was predicted to occur when $(K_{app,max} + K_{RS})$ exceeded K_{Ic} and crack arrest was predicted to occur when ΔK_w was below ΔK_{th}. Values assumed for K_{Ic} and ΔK_{th} were those for 300M, 57 MPa$\sqrt{m}$ and 4 MPa$\sqrt{m}$, respectively. The modeled applied cyclic load was constant amplitude bending with an applied stress ratio of 0.1.

The results of the AFGROW analyses are illustrated in Figure 6. AC and LP runouts were predicted to occur at maximum stress levels of 352 and 1055 MPa, respectively, which are in good agreement with the test results, and show a very large benefit from laser shock peening.

While the compressive RS case layer from carburization provides benefit for X-2M, the present testing and analysis shows that the higher magnitude and slightly deeper compression introduced by LP significantly improves the tolerance of X-2M to FOD of this size.

Acknowledgements
Funding for this work was provided through DLA contract L10457. Laser shock peening was performed at Lawrence Livermore National Laboratory. This work was carried out under the auspices of the U.S. Department of Energy by the University of California, Lawrence Livermore National Laboratory under contract no. E-7405-Eng-48. The authors would like to thank Dale Weires of the Boeing Company for his technical advice.

Tables

C	Cr	Fe	Mn	Mo	Si	V	W
0.15	5	92	0.5	1.4	0.9	0.5	1.35

Table 1 – Chemical composition of X-2M, by weight percent [9]

	S_u (MPa)	S_y (MPa)	E (GPa)
X-2M	1310-1551	1138-1172	216.5

Table 2 – Core mechanical properties of X-2M [9]

Coupon ID	FOD	Treatment	Test Load (MPa)	Lifetime (Cycles)	Failure Location
1	X	LP	145	127,672	Not at FOD
2	X	LP	140	458,787	FOD
3	X	LP	135	361,853	FOD
4	X	LP	120	1,000,000	Runout
5	X	LP	130	1,000,000	Runout
6	X	AC	55	725,456	FOD
8	X	AC	55	1,000,000	Runout
10	X	AC	60	1,000,000	Runout
12	X	AC	70	324,065	FOD
14	X	AC	65	519,966	FOD
7		AC	Dynamic Calibration Coupon		
9		AC	Spare		
11		AC	Spare		
13		AC	Spare		
15		AC	Spare		

Table 3 – Coupon treatment and test conditions

Figures

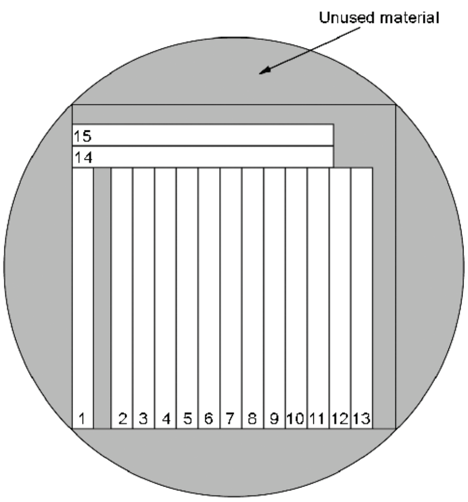

Figure 1 – Coupon location in parent material

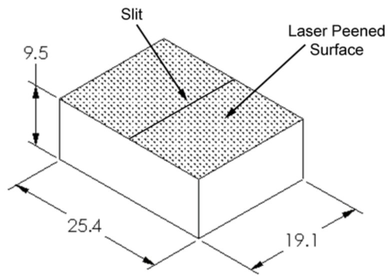

Figure 2 – Residual stress coupon, dimensions in mm

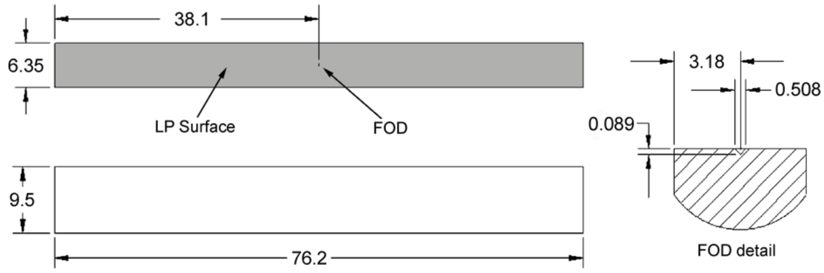

Figure 3 – Fatigue coupon and simulated damage, dimensions in mm

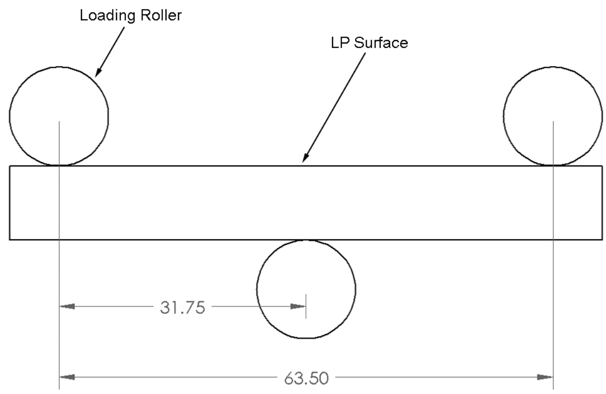

Figure 4 – Three-point bend loading of the fatigue coupon, dimensions in mm

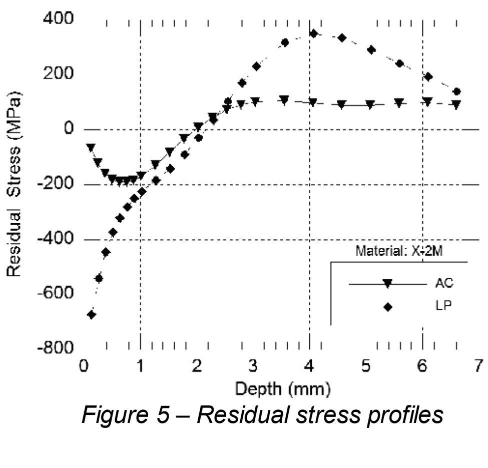

Figure 5 – Residual stress profiles

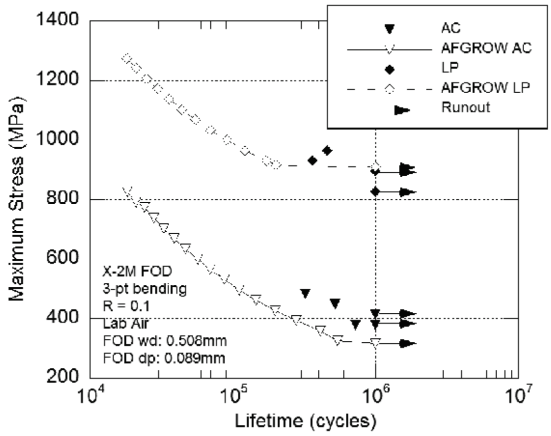

Figure 6 – Fatigue test results and AFGROW analysis

References

[1] Mall, S., Hamrick, J. L., Nicholas, T., 2001, "High Cycle Fatigue Behavior of Ti-6Al-4V with Simulated Foreign Object Damage," *Mech. of Materials*, **33**, pp. 679-692.

[2] Chen, X., 2005, "Foreign Object Damage on the Leading Edge of Thin Blade," *Mech. of Materials*, **37**, pp. 447-457.

[3] Peters J.O., Ritchie R.O., 2000, "Influence of foreign-object damage on crack initiation and early crack growth during high-cycle fatigue of Ti-6Al-4V," *Engineering Fracture Mechanics*, **67**, pp. 193-2007.

[4] Montross, C. S., Wei, T., Ye, L., Clark, G., and Mai, Y.-W., 2002, "Laser shock processing and its effects on microstructure and properties of metal alloys: a review," *International Journal of Fatigue*, **24**, pp. 1021-1036.

[5] Shepard, M. J., 2005, "Laser Shock Processing: Applications and Future Trends in US Air Force Service," American Society of Mechanical Engineers, Pressure Vessels and Piping Division (Publication) PVP, **v 7**, Proceedings of the ASME Pressure Vessels and Piping Conference 2005 - Operations, Applications and Components, PVP2005, 2005, p 215-220.

[6] Prevey, P.S., Ravindranath, R. A., Jayaraman, N., Shepard, M., "Improved High Cycle Fatigue Damage Tolerance of Turbine Engine Compressor Components by Low Plasticity Burnishing (LPB)," *Proceedings of the ASME Turbo Expo*, **v 4**, *Proceedings of the ASME Turbo Expo 2006 - Power for Land, Sea, and Air*, 2006, p 985-990

[7] Altenberger, I., Noster, U., Boyce, B. L., Peters, J. O., Scholtes, B., and Ritchie, R. O., 2002, "Effects of Mechanical Surface Treatment on Fatigue Failure in Ti-6Al-4V: Role of Residual Stresses and Foreign-object Damage," *Materials Sci. Forum*, **404**, pp. 457-462.

[8] Fabbro, R., Peyre, P., Berthe, L., and Scherpereel, X., 1998, "Physics and applications of laser-shock processing," *Journal of Laser Applications*, **10**, pp. 265-279.

[9] Alleghany Technologies Inc, Allvac Vasco X-2M info webpage

[10] Pistochini, T., M.S. Thesis, "Fatigue Life Optimization in Laser Peened 7050-T7451 and 300M Steel," Department of Mechanical and Aeronautical Engineering, University of California, Davis. 2003.

[11] Vaidynathan, S., and Finnie, I., 1971, "Determination of Residual Stress from Stress Intensity Factor Measurements," *J. Basic. Eng.*, **93**, pp. 242-246.

[12] Prime, M., 1999, "Residual stress measurement by successive extension of a slot: The crack compliance method", *Appl. Mech. Rev.*, **52**(2), pp. 75-96.

[13] Lee, M., and Hill, M., 2007, "Effect of Strain Gage Length When Determining Residual Stress By Slitting," *J. of Eng. Materials and Tech.*, **129**, pp.143-150.